

# VISUAL RHYTHM-BASED TIME SERIES ANALYSIS FOR PHENOLOGY STUDIES

*Jurandy Almeida*<sup>1</sup>, *Jefersson A. dos Santos*<sup>1</sup>, *Bruna C. Alberton*<sup>2</sup>,  
*Leonor Patricia C. Morellato*<sup>2</sup>, and *Ricardo da S. Torres*<sup>1</sup>

<sup>1</sup> RECOD Lab, Institute of Computing, University of Campinas – UNICAMP  
13083-852, Campinas, SP – Brazil

Email: {jurandy.almeida, jsantos, rtorres}@ic.unicamp.br

<sup>2</sup> Phenology Lab, Dept. of Botany, Sao Paulo State University – UNESP  
13506-900, Rio Claro, SP – Brazil

Email: bru.alberton@gmail.com, pmorella@rc.unesp.br

## ABSTRACT

Plant phenology has gained importance in the context of global change research, stimulating the development of new technologies for phenological observation. In this context, digital cameras have been successfully used as multi-channel imaging sensors, providing measures to estimate changes on phenological events, such as leaf flushing and senescence. We monitored leaf-changing patterns of a cerrado-savanna vegetation by taken daily digital images. For that, we extract leaf color information and correlated with phenological changes. In this way, time series associated with plant species are obtained, raising the need of using appropriate tools for mining patterns of interest. In this paper, we present a novel approach for representing phenological patterns of plant species. The proposed method is based on encoding time series as a visual rhythm, which is characterized by color description algorithms. A comparative analysis of different descriptors is conducted and discussed. Experimental results show that our approach presents high accuracy on identifying plant species.

*Index Terms*— remote phenology; digital cameras; image analysis; time series; visual rhythm

## 1. INTRODUCTION

Plant phenology has gained importance as the simplest and most reliable indicator of species responses in the context of global change research, stimulating the development of new technologies for phenological observation [1–5]. In this context, digital cameras have been successfully used as multi-channel imaging sensors, and the measurements of color change information (RGB channels) from digital images allow to detect changes on phenological events, such as leaf flushing and senescence [5–10].

We have been monitoring leaf-changing patterns of a tropical cerrado-savanna vegetation by taken daily digital images [11]. For that, we extracted leaf color information from the RGB channels and correlated the changes in pixel levels over time with leaf phenology patterns. The image analysis was conducted by defining regions of interest based on the random selection of plant species identified in the digital image. Time series associated with different regions in the images have been obtained, raising the need of using appropriate tools for mining patterns of interest.

In this paper, we present a novel approach for capturing phenological patterns from time series and distinguishing the behavior of plant species. It relies on encoding time series as a visual rhythm [18], which is characterized by traditional and recently proposed color description algorithms. This computationally simple approach opens a new area of investigation related to the use of image descriptors to identify and characterize phenological changes.

We evaluate the proposed algorithm on about 2,700 images, recorded during the main leaf flushing season [11]. Results from a detailed experimental comparison of several descriptors show that our method presents high accuracy on identifying regions in the images belonging to a same plant species.

The remainder of this paper is organized as follows. Section 2 briefly describes related work. Section 3 discusses the methodology adopted for acquiring time series. Section 4 presents our approach and shows how to apply it to characterize time series. Section 5 reports the results of our experiments and compares our technique with other methods. Finally, we offer our conclusions and directions for future work in Section 6.

## 2. RELATED WORK

The increasing accessibility to data with high spatio-temporal resolution has enabled a detailed analysis of vegetation properties. At the same time, it requires feature extraction techniques able to properly represent such properties, taking into account storage aspects.

Time series based on vegetation indexes are the most common features extracted from remote sensing images (RSIs) for phenological and land cover change studies [12–14]. Rodrigues *et al.* [13] presented a software to extract phenological parameters (e.g., maturity and senescence) from Normalized Difference Vegetation Index (NDVI) time series. Foster *et al.* [12] also applied NDVI time series to detect grassland vegetation. Brooks *et al.* [14], in turn, proposed a Fourier-based algorithm to fit NDVI multitemporal curves and reduce missing data effects in the analysis.

In [15–17], the authors consider not only temporal but also spatial properties. For that, they extract time series from segmented regions. Petitjean *et al.* [15] proposed a strategy to encode spatial data along the time. Their strategy consists in segmenting each image of the series in order to characterize each pixel of the data with spatial properties. The time series are computed for each pixel based on the properties extracted from the segmented regions. Ardila *et al.* [16],

---

Thanks to CAPES, CNPq, FAPESP, and Microsoft Research for funding.

in turn, used time series based on spatial properties from pre-defined regions to monitor urban trees. Almeida *et al.* [17] exploited a multiscale segmentation structure to compute time series with spatial information, which were used to detect phenological patterns in a cerrado-savanna vegetation.

Different from those initiatives, this paper addresses efficiency issues involved in time series analysis. In spite of all the advances, existing strategies for processing spatio-temporal data usually require a huge amount of storage space. Here, we introduce a compact representation for identifying and characterizing plant species in time series obtained from phenological observations.

### 3. TIME SERIES ACQUISITION

The near-remote phenological system was set up in a 18m tower in a Cerrado *sensu stricto*, a savanna-like vegetation located at Itirapina, São Paulo State, Brazil. A digital hemispherical lens camera (Mobotix Q24) was setup at the top of the phenology tower, attached in an iron arm facing northeast.

The first data collection from the digital camera started on 18th August 2011. We set up the camera to automatically take a daily sequence of five JPEG images (at  $1280 \times 960$  pixels of resolution) per hour, from 6:00 to 18:00 h (UTC-3). The present study was based on the analysis of over 2,700 images (Figure 1), recorded at the end of the dry season, between August 29th and October 3rd 2011, day of year 241 to 278, during the main leaf flushing season [11].



**Fig. 1.** Sample image of the cerrado savanna recorded by the digital camera on October 15th, 2011.

The image analysis was conducted by defining different regions of interest (ROI), as described by Richardson *et al.* [5], Richardson *et al.* [6], and Ahrends *et al.* [7]. We defined six ROIs (Figure 2) based on the random selection of six plant species identified in the hemispheric image: (1) *Aspidosperma tomentosum* (Figure 2(a)), (2) *Caryocar brasiliensis* (Figure 2(b)), (3) *Myrcia guianensis* (Figure 2(c)), (4) *Miconia rubiginosa* (Figure 2(d)), (5) *Pouteria ramiflora* (Figure 2(e)), and (6) *Pouteria torta* (Figure 2(f)).

### 4. VISUAL RHYTHM-BASED DESCRIPTION

Visual rhythms [18] are an effective way to analyze temporal properties from video data. It consists in an abstraction of a video that encodes the temporal change of pixel values along a specific sampling line [19], as illustrated in Figure 3(a). A clear advantage of this approach is to reduce the storage space of the extracted features. Therefore, it also speeds up data processing.

Formally, a visual rhythm is a simplification of a video  $\mathcal{V} = \{f_t\}, t \in [1, T]$ , in domain  $2D + t$ , with  $T$  frames of dimensions  $W_{\mathcal{V}} \times H_{\mathcal{V}}$ , in which each frame  $f_t$  is transformed into a vertical line on an image  $\mathcal{R}$ , in domain  $1D + t$ , such that,

$$\mathcal{R}(t, z) = f_t(r_x \times z + a, r_y \times z + b), t \in [1, W_{\mathcal{R}}], z \in [1, H_{\mathcal{R}}],$$

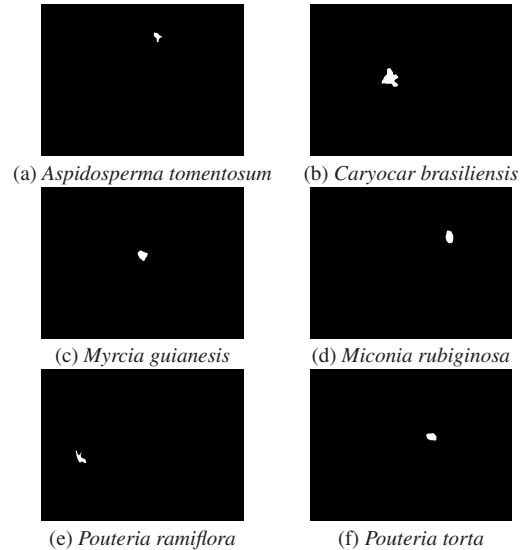


**Fig. 2.** Regions of interest (ROIs) defined for the analysis of six plant species from the cerrado-savanna vegetation.

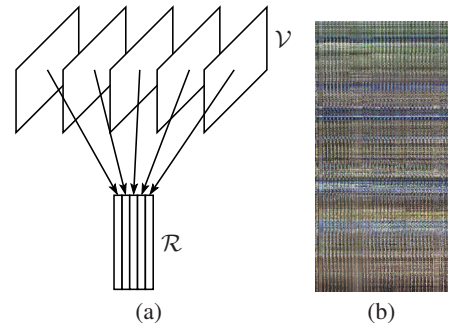


**Fig. 3.** Visual rhythm: (a) simplification of a video content by mapping each frame into one column of an image; (b) a real example produced by sampling the central vertical line of the digital images.

where  $W_{\mathcal{R}} = T$  and  $H_{\mathcal{R}}$  are its width and height,  $r_x$  and  $r_y$  are the sampling rates along the horizontal and vertical directions,  $a$  and  $b$  are the horizontal and vertical offsets on each frame, respectively.

Without loss of generality, a time series comprised of images taken by digital cameras at fixed time intervals can be viewed as a video of the vegetation. Thus, a visual rhythm can be used to simplify a time series into a single image, as illustrated in Figure 3(b). In this way, we can take the advantage of existing image descriptors to identify and characterize phenological changes.

The major problem with the previous definition of visual rhythms is to have been designed for the pixel sampling of specific lines (e.g., diagonal, horizontal, and vertical). Here, we are interested in analyzing unshapely regions related to plant species that are identified by phenology experts (see Figure 2). However, it is impossible to adjust values for the parameters  $r_x$ ,  $r_y$ ,  $a$ , and  $b$  so that we can transform a ROI into a vertical line of a visual rhythm.

The novelty of this paper is to generalize the notion of visual rhythms. From a generic point of view, this approach relies on taking samples of the information to be analyzed and then grouping them in an orderly manner. The key contribution of our idea is the mapping function we design to transform a ROI into a vertical line.

Let  $\mathcal{V} = \{f_t\}, t \in [1, T]$  be a video, in domain  $2D + t$ , with  $T$  frames of dimensions  $W_V \times H_V$ ; and  $\mathcal{I}$  be a binary image, with the same dimensions of  $\mathcal{V}$ , in which white pixels indicate a ROI.

Initially, we convert the image  $\mathcal{I}$  into a list of Cartesian coordinates  $\mathcal{L}_{xy} = \{(x, y) \mid \mathcal{I}(x, y) = 1\}$ . Next, we use this list for computing the geometric center  $(x_c, y_c)$  of the ROI. After that, we translate the Cartesian coordinate system of the elements in the list  $\mathcal{L}_{xy}$  to have its origin at the point  $(x_c, y_c)$  and then we convert them to the polar coordinate system, creating a list of polar coordinates  $\mathcal{L}_{r\theta}$ . Thereafter, we create an index  $\mathcal{K} = \{k \mid \forall (r, \theta) \in \mathcal{L}_{r\theta}, k = 2\pi r + \theta\}$  which assigns a unique value to each element in the list  $\mathcal{L}_{r\theta}$ . Finally, we sort the keys in the index  $\mathcal{K}$  in an increasing order and then we use them to arrange the elements in the list  $\mathcal{L}_{xy}$ .

Thus, we can define a visual rhythm as a mapping of each frame  $f_t$  into a vertical line on an image  $\mathcal{R}^*$ , in domain  $1D + t$ , such that

$$\mathcal{R}^*(t, z) = f_t(\mathcal{L}_{xy}(z)), t \in [1, W_{\mathcal{R}^*}], z \in [1, H_{\mathcal{R}^*}],$$

where  $W_{\mathcal{R}^*} = T$  and  $H_{\mathcal{R}^*} = |\mathcal{L}_{xy}|$  are its width and height, respectively. Figure 4 presents the visual rhythms produced by the pixel sampling of the digital images using each ROI from Figure 2.

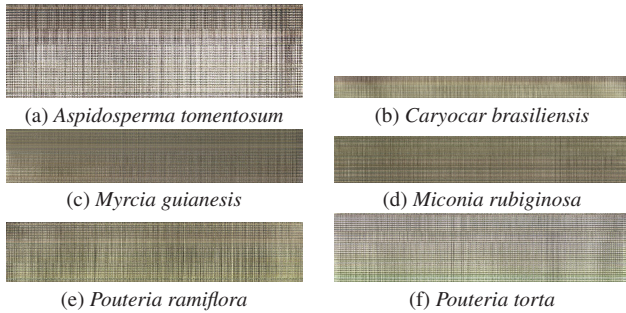


Fig. 4. Visual rhythms obtained for each ROI.

## 5. EXPERIMENTS AND RESULTS

We carried out experiments to identify the plant species in the image. For describing time series encoded into a visual rhythm, we used four traditional and recently proposed color descriptors: ACC [20], CCV [21], BIC [22], and GCH [23]. The distance function used for feature comparison is the Manhattan ( $L_1$ ) distance.

Our strategy to evaluate color descriptors in the context of time series description is based on assessing the similarity among regions associated with individuals of the same species. Regions are defined by using the hierarchical segmentation based on the Guigues algorithm [24]. The image used to obtain the hierarchy of segmented regions was taken at noon on October 15th, 2011 (Figure 1). We have selected 5 segmentation scales from the hierarchy to perform feature extraction. The finest scale is composed of 27,380 regions and the coarsest scale contains 8,849 regions. Figure 5 illustrates the segmented scales in a subimage sample.

The similarity between two regions is computed as a function of the distance between the feature vectors extracted from their visual rhythms. A color descriptor is better than another if it ranks more regions belonging to the same ROI of an input region at the first positions. We consider a given region as belonging to a ROI if at least 80% of its size is overlapped by such a ROI. In our experiments, we have used only regions from the coarsest scale, as they have been shown the most effective ones to characterize plant species [17].

For each ROI, we randomly selected twenty percent of its total number of regions to be used as queries. Five replications were

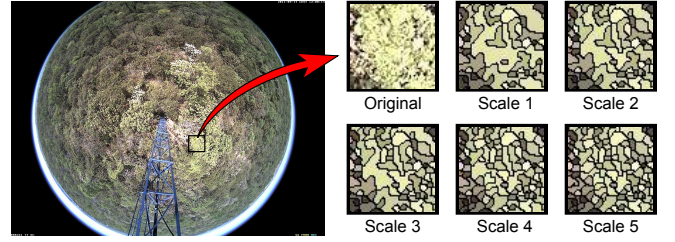


Fig. 5. Segmentation results for each of the scales in a image sample.

performed in order to ensure statistically sound results. Presented results consider the average performance of the evaluated color descriptors, which were computed based on the mean and standard deviation of each replication.

We assess the effectiveness of each approach using the metrics of Precision and Recall. Precision is the ratio of the number of relevant regions retrieved to the total number of irrelevant and relevant regions retrieved. Recall is the ratio of the number of relevant regions retrieved to the total number of relevant regions in the database. Here, a given region is considered as relevant only if it belongs to the same ROI of a query region.

However, there is a trade-off between Precision and Recall. Greater Precision decreases Recall and greater Recall leads to decreased Precision. So, we choose to report the results using unique-value measurements: Mean Average Precision (MAP), which is the mean of the precision scores obtained at the ranks of each relevant region; and Precision at 5 (P@5), which is the average precision after 5 regions are returned. These metrics combine both Precision and Recall into a single measure, which makes the comparison easier.

Our experiments are intended to: i) analyze the impact of the sunshine on the performance of color descriptors and ii) determine which color descriptor is better for characterizing plant species. In those experiments, we compare the visual rhythm-based techniques with the method proposed by Richardson *et al.* [6], which is the most popular approach and widely used by the phenology community for characterizing phenological patterns of plant species. It consists in analyzing each region in terms of the variation of the relative (or normalized) brightness of the primary colors (RGB channels).

In Tables 1 and 2, we compare the visual rhythm-based techniques and the baseline method with respect to the MAP and P@5 measures, respectively. MAP is a good indication of the effectiveness considering all positions of obtained ranked lists. P@5, in turn, focuses on the effectiveness of the methods considering only the first positions of the ranked lists. For each approach, we highlight the hour of the day that provided the best result.

Those results indicate that the performance of the different evaluated approaches is similar, with a small advantage to the baseline method. Notice that early hours (from 8h to 11h) are better to characterize the phenological changes of plant species by using color descriptors. As we can observe, the best performances were achieved using the digital images taken at ten in the morning. This finding disagrees with the general suggestion of extracting color information from midday hours (from 11h to 14h) for ecological studies [5–8].

Paired  $t$ -tests were performed to verify the statistical significance of those results. For that, the confidence intervals for the differences between paired means of each ROI were computed to compare every pair of approaches. If the confidence interval includes zero, the difference is not significant at that confidence level. If the confidence interval does not include zero, then the sign of the difference indicates which alternative is better [25].

**Table 1.** MAP scores obtained by each of the color descriptors along all the available periods of the day.

Hour	ACC	BIC	CCV	GCH	RGB
6	0.595	0.591	0.581	0.591	0.608
7	0.584	0.592	0.578	0.587	0.629
8	0.610	0.592	0.565	0.588	0.614
9	0.615	0.598	0.571	0.590	0.628
10	<b>0.658</b>	<b>0.643</b>	<b>0.608</b>	<b>0.640</b>	0.623
11	0.612	0.608	0.566	0.604	0.626
12	0.546	0.536	0.517	0.532	0.616
13	0.559	0.522	0.506	0.515	0.647
14	0.583	0.555	0.531	0.529	0.665
15	0.578	0.552	0.532	0.521	<b>0.680</b>
16	0.549	0.536	0.514	0.510	0.660
17	0.545	0.530	0.510	0.513	0.618
18	0.592	0.597	0.597	0.591	0.631

**Table 2.** P@5 scores obtained by each of the color descriptors along all the available periods of the day.

Hour	ACC	BIC	CCV	GCH	RGB
6	0.763	0.768	0.751	0.758	0.869
7	0.836	0.815	0.791	0.814	<b>0.871</b>
8	0.812	0.806	0.746	0.804	0.780
9	0.828	0.806	0.756	0.780	0.824
10	<b>0.850</b>	<b>0.848</b>	<b>0.799</b>	<b>0.849</b>	0.831
11	0.825	0.824	0.757	0.798	0.800
12	0.754	0.764	0.734	0.775	0.780
13	0.820	0.780	0.734	0.744	0.813
14	0.821	0.769	0.751	0.769	0.860
15	0.811	0.754	0.733	0.716	0.866
16	0.740	0.729	0.714	0.712	0.828
17	0.762	0.739	0.713	0.757	0.817
18	0.768	0.777	0.763	0.751	0.796

Tables 3 and 4 present the 95% confidence intervals of the differences between the baseline method and the visual rhythm-based techniques for the MAP and P@5 measures, respectively. For simplicity and readability purposes, we report only the results for the hour of the day that provided the best result of each approach.

**Table 3.** Differences between MAP of the different approaches.

Approach	Confidence Interval (95%)	
	min.	max.
RGB@15h - ACC@10h	<b>-0.112</b>	0.222
RGB@15h - BIC@10h	<b>-0.138</b>	0.278
RGB@15h - CCV@10h	<b>-0.108</b>	0.323
RGB@15h - GCH@10h	<b>-0.123</b>	0.283

**Table 4.** Differences between P@5 of the different approaches.

Approach	Confidence Interval (95%)	
	min.	max.
RGB@7h - ACC@10h	<b>-0.011</b>	0.106
RGB@7h - BIC@10h	<b>-0.052</b>	0.092
RGB@7h - CCV@10h	<b>-0.029</b>	0.190
RGB@7h - GCH@10h	<b>-0.017</b>	0.116

Such analyses confirms that the visual rhythm-based techniques and the baseline method exhibit similar performance. Notice that the confidence intervals include zero and, hence, the differences between those approaches are not significant at that confidence level.

In Tables 5 and 6, we compare the individual scores obtained for each ROI considering the best results of the evaluated methods in terms of the MAP and P@5 measures, respectively. For each ROI, we highlight the approach that provided the highest score.

**Table 5.** MAP scores obtained for each ROI.

ROI	ACC	BIC	CCV	GCH	RGB
<i>A. tomentosum</i>	0.684	0.574	0.522	0.594	<b>0.989</b>
<i>C. brasiliensis</i>	0.749	<b>0.774</b>	0.763	0.767	0.660
<i>M. guianensis</i>	0.469	0.457	0.425	0.405	<b>0.723</b>
<i>M. rubiginosa</i>	0.653	0.646	0.611	<b>0.709</b>	0.683
<i>P. ramiflora</i>	<b>0.523</b>	0.465	0.378	0.461	0.464
<i>P. torta</i>	0.528	<b>0.584</b>	0.538	0.494	0.472

**Table 6.** P@5 scores obtained for each ROI.

ROI	ACC	BIC	CCV	GCH	RGB
<i>A. tomentosum</i>	0.920	0.903	0.714	0.920	<b>1.000</b>
<i>C. brasiliensis</i>	<b>0.909</b>	0.893	0.891	0.904	0.895
<i>M. guianensis</i>	0.752	0.792	<b>0.824</b>	0.728	0.808
<i>M. rubiginosa</i>	0.770	0.750	0.770	0.820	<b>0.870</b>
<i>P. ramiflora</i>	0.755	<b>0.760</b>	0.635	<b>0.760</b>	0.745
<i>P. torta</i>	0.640	<b>0.840</b>	0.680	0.600	0.760

It is interesting to note the differences in responsiveness of the different evaluated methods with respect to each of the species individually. The main reason for those results is the different patterns of the leaf color change of each species. In general, different color descriptors are designed to capture different visual features.

The key advantage of our technique is its computational efficiency. Table 7 presents the computational cost and the space requirements (in terms of the length  $n$  of the time series) of all the compared methods. In this way, we can investigate the relative difference of performance among different approaches.

**Table 7.** The computational cost and the space requirements of the different approaches.

Approach	Computational Cost		Space Requirements
	Extraction	Matching	
VR + ACC	$O(n)$	$O(1)$	$O(1)$
VR + BIC	$O(n)$	$O(1)$	$O(1)$
VR + CCV	$O(n)$	$O(1)$	$O(1)$
VR + GCH	$O(n)$	$O(1)$	$O(1)$
RGB	$O(n)$	$\Omega(n)$	$\Omega(n)$

Clearly, the visual rhythm-based techniques are much more efficient than the current solution. This improvement makes our approach suitable for long-term collections of image data.

## 6. CONCLUSIONS

In this paper, we have presented a novel approach for capturing phenological patterns from time series and distinguishing the behavior of plant species. Our technique relies on encoding time series as a visual rhythm, which is characterized by image descriptors. Such a combination makes our method suitable for long-term temporal data.

We have validated our technique using about 2,700 images, taken from a tropical cerrado-savanna vegetation, including a high diversity of plant species. Results from the application of our method with several color descriptors show that it presents high accuracy on identifying regions in the images belonging to a same species.

Future work includes the evaluation of other visual features for image retrieval (e.g., local features [26]). In addition, the proposed method can be augmented to consider temporal segmentation [27] and/or summarization methods [28,29]. Finally, we also plan to consider learning-to-rank methods (e.g., genetic programming [30]) for combining different descriptors.

## 7. REFERENCES

- [1] G. R. Walther, E. Post, P. Convey, A. Menzel, C. Parmesan, T. J. C. Beebee, J. M. Fromentin, O. Hoegh-Guldberg, and F. Bairlein, "Ecological responses to recent climate change," *Nature*, vol. 416, pp. 389–395, 2002.
- [2] C. Parmesan and G. A. Yohe, "A globally coherent fingerprint to climate change impacts across natural systems," *Nature*, vol. 421, pp. 37–42, 2003.
- [3] G. R. Walther, "Plants in a warmer world," *Perspectives in Plant Ecology Evolution and Systematics*, vol. 6, pp. 169–185, 2004.
- [4] C. Rosenzweig, D. Karoly, M. Vicarelli, P. Neofotis, Q. Wu, G. Casassa, A. Menzel, T. L. Root, N. Estrella, B. Seguin, P. Tryjanowski, C. Liu, S. Rawlins, and A. Imeson, "Attributing physical and biological impacts to anthropogenic climate change," *Nature*, vol. 453, pp. 353–357, 2008.
- [5] A. D. Richardson, B. H. Braswell, D. Y. Hollinger, J. P. Jenkins, and S. V. Ollinger, "Near-surface remote sensing of spatial and temporal variation in canopy phenology," *Ecological Applications*, vol. 19, pp. 1417–1428, 2009.
- [6] A. D. Richardson, J. P. Jenkins, B. H. Braswell, D. Y. Hollinger, S. V. Ollinger, and M. L. Smith, "Use of digital webcam images to track spring greening-up in a deciduous broadleaf forest," *Oecologia*, vol. 152, pp. 323–334, 2007.
- [7] H. Ahrends, S. Etzold, W. Kutsch, R. Stoeckli, R. Bruegger, F. Jeanneret, H. Wanner, N. Buchmann, and W. Eugster, "Tree phenology and carbon dioxide fluxes: Use of digital photography for process-based interpretation at the ecosystem scale," *Climate Research*, vol. 39, pp. 261–274, 2009.
- [8] R. Ide and H. Oguma, "Use of digital cameras for phenological observations," *Ecological Informatics*, vol. 5, pp. 339–347, 2010.
- [9] S. Kurc and L. Benton, "Digital image-derived greenness links deep soil moisture to carbon uptake in a creosotebush-dominated shrubland," *Journal of Arid Environments*, vol. 74, pp. 585–594, 2010.
- [10] S. Nagai, T. Maeda, M. Gamo, H. Muraoka, R. Suzuki, and K. N. Nasahara, "Using digital camera images to detect canopy condition of deciduous broad-leaved trees," *Plant Ecology and Diversity*, vol. 4, pp. 79–89, 2011.
- [11] B. Alberton, J. Almeida, R. Henneken, R. S. Torres, A. Menzel, and L. P. C. Morellato, "Near remote phenology: Applying digital images to monitor leaf phenology in a brazilian cerrado savanna," in *Int. Conf. Phenology (Phenology'12)*, 2012, p. 2.
- [12] M. Forster, T. Schmidt, C. Schuster, and B. Kleinschmit, "Multi-temporal detection of grassland vegetation with rapid-eye imagery and a spectral-temporal library," in *IEEE Int. Symp. Geoscience and Remote Sensing (IGARSS'12)*, 2012, pp. 4930–4933.
- [13] A. Rodrigues, A. R. S. Marcal, and M. Cunha, "Phenology parameter extraction from time-series of satellite vegetation index data using phenosat," in *IEEE Int. Symp. Geoscience and Remote Sensing (IGARSS'12)*, 2012, pp. 4926–4929.
- [14] E. B. Brooks, V. A. Thomas, R. H. Wynne, and J. W. Coulston, "Fitting the multitemporal curve: A fourier series approach to the missing data problem in remote sensing analysis," *IEEE Transactions on Geoscience and Remote Sensing*, vol. 50, no. 9, pp. 3340–3353, 2012.
- [15] F. Petitjean, C. Kurtz, N. Passat, and P. Ganarski, "Spatio-temporal reasoning for the classification of satellite image time series," *Pattern Recognition Letters*, vol. 33, no. 13, pp. 1805–1815, 2012.
- [16] J. P. Ardila, W. Bijker, V. A. Tolpekin, and A. Stein, "Multitemporal change detection of urban trees using localized region-based active contours in vhr images," *Remote Sensing of Environment*, vol. 124, pp. 413–426, 2012.
- [17] J. Almeida, J. A. Santos, B. Alberton, R. S. Torres, and L. P. C. Morellato, "Remote phenology: Applying machine learning to detect phenological patterns in a cerrado savanna," in *IEEE Int. Conf. eScience (eScience'12)*, 2012, pp. 1–8.
- [18] C. W. Ngo, T. C. Pong, and R. T. Chin, "Detection of gradual transitions through temporal slice analysis," in *IEEE Int. Conf. Computer Vision and Pattern Recognition (CVPR'99)*, 1999, pp. 1036–1041.
- [19] J.-S. Lee and T. Ebrahimi, "Perceptual video compression: A survey," *IEEE Journal of Selected Topics in Signal Processing*, vol. 6, no. 6, pp. 684–697, 2012.
- [20] J. Huang, R. Kumar, M. Mitra, W.-J. Zhu, and R. Zabih, "Image indexing using color correlograms," in *IEEE Int. Conf. Computer Vision and Pattern Recognition (CVPR'97)*, 1997, pp. 762–768.
- [21] G. Pass, R. Zabih, and J. Miller, "Comparing images using color coherence vectors," in *ACM Int. Conf. Multimedia (ACM-MM'96)*, 1996, pp. 65–73.
- [22] R. O. Stehling, M. A. Nascimento, and A. X. Falcão, "A compact and efficient image retrieval approach based on border/interior pixel classification," in *ACM Int. Conf. Information and Knowledge Management (CIKM'02)*, 2002, pp. 102–109.
- [23] M. J. Swain and B. H. Ballard, "Color indexing," *International Journal of Computer Vision*, vol. 7, no. 1, pp. 11–32, 1991.
- [24] L. Guigues, J. Cocquerez, and H. Le Men, "Scale-sets image analysis," *International Journal of Computer Vision*, vol. 68, pp. 289–317, 2006.
- [25] R. Jain, *The Art of Computer Systems Performance Analysis: Techniques for Experimental Design, Measurement, Simulation, and Modeling*, John Wiley and Sons, Inc., 1991.
- [26] J. Almeida, A. Rocha, R. S. Torres, and S. Goldenstein, "Making colors worth more than a thousand words," in *ACM Int. Symp. Applied Computing (ACM-SAC'08)*, 2008, pp. 1180–1186.
- [27] J. Almeida, N. J. Leite, and R. S. Torres, "Rapid cut detection on compressed video," in *Iberoamerican Congress on Pattern Recognition (CIARP'11)*, 2011, pp. 71–78.
- [28] J. Almeida, R. S. Torres, and N. J. Leite, "Rapid video summarization on compressed video," in *IEEE Int. Symp. Multimedia (ISM'10)*, 2010, pp. 113–120.
- [29] J. Almeida, N. J. Leite, and R. S. Torres, "VISON: VIdeo Summarization for ONline applications," *Pattern Recognition Letters*, vol. 33, no. 4, pp. 397–409, 2012.
- [30] F. S. P. Andrade, J. Almeida, H. Pedrini, and R. S. Torres, "Fusion of local and global descriptors for content-based image and video retrieval," in *Iberoamerican Congress on Pattern Recognition (CIARP'12)*, 2012, pp. 845–853.